

Reduced SnO₂ surfaces by first-principles calculations

Wolfgang Bergmayer^{a)}

Fukui Institute for Fundamental Chemistry, Kyoto University, Sakyo, Kyoto, 606-8103 Japan

Isao Tanaka

Department of Materials Science and Engineering, Kyoto University, Sakyo, Kyoto, 606-8501 Japan

(Received 6 October 2003; accepted 12 December 2003)

SnO₂(110) and (101) surfaces with eleven different kinds of terminations for each are systematically investigated by a first-principles projector augmented wave method. Surface energies are discussed as a function of temperature and oxygen partial pressure. Atomic relaxations of the surfaces are then compared. In agreement with previous calculations, the stoichiometric (110) surface is the most stable surface at high oxygen chemical potentials (i.e., low temperature or high pressure). At lower oxygen chemical potentials, however, one of the reduced (101) surface terminations becomes energetically preferred. The other surface terminations are found to be less stable. This is consistent with recent thin-film experimental results. © 2004 American Institute of Physics. [DOI: 10.1063/1.1646460]

Tin dioxide or stannic oxide with the rutile structure, known under the mineralogical name cassiterite, is a wide gap (3.6 eV) material. Due to its electronic structure and the possibility of two different oxidation states (+2,+4) of Sn, SnO₂ is very sensitive to oxidizing and reducing gases. It is therefore used in many applications, such as oxidation catalyst and gas sensor. Upon reaction of these gases with the SnO₂ surface, a change of conductivity can be measured. A lot has been published about SnO₂ surfaces. However, most studies concentrated on the SnO₂(110) surface, e.g., Refs. 1–3. Recently, some experimental studies have claimed that the SnO₂(101) surface should also be stable under certain experimental conditions.^{4,5} In this context, we perform *ab initio* calculations of both the SnO₂(110) and the SnO₂(101) surfaces and compare the results. As we have to take into account various experimental conditions and, therefore, different temperature and pressure ranges, we will study the dependence of the surface energy on the chemical potential. In this way, we can predict the most stable surface termination for a given partial pressure of oxygen and the temperature of the system.

Our calculations are based on density functional theory using the generalized gradient approximation (GGA) for the exchange-correlation potential as given by Perdew and Wang (1991).^{6,7} The Kohn–Sham equations are solved with a plane wave basis as implemented in the VASP code^{8–10} with its projector augmented wave (PAW) potentials.^{11,12} The PAW Sn potential is given for 14 valence electrons of the configuration $4d^{10}5s^25p^2$, the O potential for six valence electrons with the configuration $2s^22p^4$. The cutoff in the plane wave expansion was taken to be 400 eV.

As a first step, the cell parameters of bulk SnO₂ are computed. For this, the *k* mesh is carefully checked leading us to the conclusion, that a *k*-point spacing of less than 0.28 Å⁻¹ is necessary to obtain convergence of the cell energy to less than 5 meV/cell. For the tetragonal SnO₂ cell, we obtain

values of $a=b=4.82$ Å and $c=3.24$ Å, which is about 1.8% larger than the experimental values. This deviation lies within the usual errors of the GGA method.

Different surface terminations of the SnO₂(110) and (101) surfaces are investigated. The oxygen coverage, structure, and thermodynamic stability of surfaces are a function of temperature and pressure. Therefore, a thermodynamic approach is mandatory. Conceptually, the physical system of the present study consists of three regions, namely a large region of bulk and stoichiometric SnO₂, a large gas phase region consisting of molecular oxygen at pressure *p*, and a surface region with chemical composition Sn_{*x*}O_{*y*} in a *a priori* unknown structure. The surface region contains a total number of N_{Sn} and N_{O} of tin and oxygen atoms, respectively. The entire system is surrounded by a thermal bath of temperature *T*. The oxygen partial pressure and the temperature are kept in a range where SnO₂ is thermodynamically stable, i.e., the oxygen partial pressure is sufficiently high and the temperature sufficiently low.

The free energy of the SnO₂ surface can be given by

$$\Omega_{\text{surface}} = G_{\text{surface}} - N_{\text{Sn}}\mu_{\text{Sn}} - N_{\text{O}}\mu_{\text{O}}, \quad (1)$$

where μ_{Sn} and μ_{O} are chemical potentials of Sn and O, which are connected by the chemical potential of bulk and stoichiometric SnO₂ $\mu_{\text{SnO}_2}^{\text{bulk}}$ as

$$\mu_{\text{Sn}} + 2\mu_{\text{O}} = \mu_{\text{SnO}_2}^{\text{bulk}}. \quad (2)$$

G_{surface} is the Gibbs free energy of the surface region, which can be given by $G = U + pV - TS$ with *U* being the internal energy. It is assumed that the terms *pV* and *TS* are similar for the different surface terminations and thus can be cancelled when relative stability among surfaces are compared. Furthermore, the internal energy *U* is approximated by the total energy of the surface region as obtained from ground-state electronic structure calculations using a supercell composed of an atomic slab, $E_{\text{slab}}^{\text{total}}$. This assumption implies that the phonon density of the solid does not depend strongly on the surface structure and composition. We have

^{a)}Electronic mail: wolfgang@fukui.kyoto-u.ac.jp

assumed that $\mu_{\text{SnO}_2}^{\text{bulk}}$ is given by the total energy per unit formula of bulk SnO_2 , $E_{\text{SnO}_2}^{\text{total}}$. Division of Ω_{surface} by the surface area, A , and accounting for the two surfaces of the slab leads to the surface free energy $\gamma = \Omega_{\text{surface}}/2A$.

The gas phase above the SnO_2 surface contains O_2 molecules. The total energy of the O_2 molecule can be related to the chemical potential of oxygen at $T=0$ K and $p=p^0$ as $1/2E_{\text{O}_2}^{\text{total}} = \mu_{\text{O}}(0, p^0)$. The chemical potential of oxygen for arbitrary T and p , $\mu_{\text{O}}(T, p)$ can be given by

$$\mu_{\text{O}}(T, p) = \mu_{\text{O}}(T, p^0) + \frac{1}{2}kT \ln\left(\frac{p}{p^0}\right). \quad (3)$$

Following common practice,¹³ the temperature dependence of μ_{O} is taken from experimental data as given in the standard thermodynamic table.¹⁴ p^0 is taken to be 1 atm. In principle, one may have to consider the temperature dependence of free energies of solids. However, the major contribution for the temperature dependence of the surface energy as given by Eq. (1) comes from the large standard entropy of O_2 gas as compared to the solid systems. Moreover, the smaller temperature dependence of chemical potentials of solids can be cancelled in Eq. (1). Therefore, only the temperature dependence of μ_{O} was taken into account in this work.

μ_{O} should be restricted by the conditions that: (i) SnO_2 does not decompose in SnO and (ii) molecular oxygen does not condense on the surface. These conditions imply $1/2E_{\text{O}_2}^{\text{total}} > \mu_{\text{O}} > E_{\text{SnO}_2}^{\text{total}} - E_{\text{SnO}}^{\text{total}}$.

The periodic unit of the surface plane of $\text{SnO}_2(110)$ is composed of two Sn and four O when the slab to model the surface is stoichiometric. It will be called Sn_2O_4 termination. By subsequent removal of O and/or Sn within the same surface periodicity, all the other terminations can be created: Sn_2O_3 , Sn_2O_2 , Sn_2O_1 , Sn_2 , Sn_1O_4 , Sn_1O_3 , Sn_1O_2 , Sn_1O_1 , and finally, Sn_3O_4 and Sn_2O_5 . These are, in sum, eleven terminations which can be constructed for both the 110 and 101 surfaces. The slabs are all set up symmetrically, so that the two surfaces of the slab are identical. Surface energies are compared after geometry optimization of all different surfaces. For the surface cells, the number of necessary layers and the necessary vacuum width have been carefully checked. We conclude, that a five layer slab for the (110) surface and a seven layer slab for the (101) surface with a vacuum width of 10 Å is sufficient to obtain results with convergence in surface energy within 5 meV/Å². The relaxations are done layer by layer, starting with the first layer and fixing the inner layers, until all layers are relaxed. The k mesh is chosen with a spacing of less than 0.5 Å⁻¹ for the relaxations, until forces become smaller than 0.01 eV/Å, and then continued with a spacing of less than 0.28 Å⁻¹.

The thermodynamic stability of the two surfaces and the eleven different surface terminations for each are compared as a function of the chemical potential of oxygen and temperature. Figure 1 shows the surface energies for stoichiometric Sn_2O_4 and reduced $\text{Sn}_2\text{O}_2(110)$ and (101) surfaces at $p_{\text{O}_2} = 10^{-7}$ atm. It is interesting that all other surface terminations show larger surface energies than either of these two cases under the conditions shown in Fig. 1. In other words, only two surface terminations of each surface play a role, all others are less stable. The relative stability of different sto-

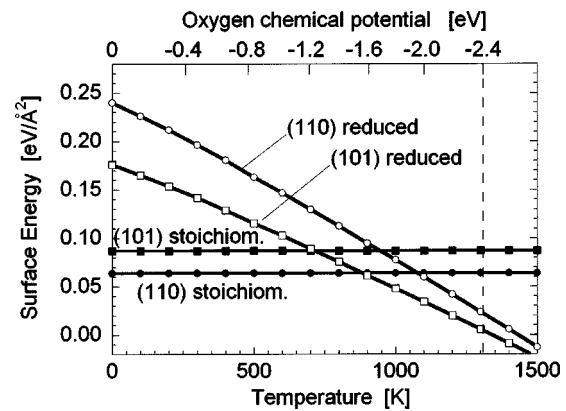


FIG. 1. Dependence of the surface energy on the temperature or oxygen chemical potential at an oxygen pressure of 10^{-7} atm. The vertical line at a potential of -2.4 eV denotes the decomposition of SnO_2 into SnO and O_2 at a temperature of around 1300 K.

ichiometric surfaces of SnO_2 has been examined by Oviedo and Gillan.¹⁵ They found that the surface energy for (110) is smaller than that for (101) by 0.29 J/m² or 18 meV/Å². Our result of 23 meV/Å² is in agreement with them. As the energy of stoichiometric surfaces depends neither on the oxygen chemical potential nor on the temperature, the stoichiometric (110) surface is more stable than the stoichiometric (101) surface for all temperature and pressure ranges. Compared to the nonstoichiometric surface terminations, the (110) Sn_2O_4 terminated surface is the most stable surface at high oxygen chemical potentials (i.e., low temperature or high pressure). At typical vacuum conditions of 10^{-7} atm, the redox occurs at a temperature of around 720 K for the (101) surface, and at 1080 K for the (110) surface. It should be mentioned that for the reduced surfaces, the (101) surface is always more stable than the (110) surface.

Oviedo and Gillan¹ have examined a reduced (110) surface of SnO_2 , where all bridged O atoms have been removed from the surface. This so called “planar-reduced surface” corresponds to the Sn_2O_3 termination in our definition. In the present calculation, this surface is found to be less stable than the reduced Sn_2O_2 or the Sn_2O_4 surface under any thermodynamical conditions. Mäki-Jaskari and Rantala¹⁶ reported relative stability and local electronic structure of ordered stoichiometric and oxygen-deficient (110) surfaces. Their results are qualitatively similar to our results of the (110) surface. However, they did not examine the (101) surface.

Dominguez *et al.*^{4,5} reported that thin films of SnO_2 made by pulsed laser deposition process on sapphire (1012) substrates at 973 K and oxygen backfill pressure of the order of 10^{-7} atm prefer to grow with (101) planes parallel to the substrate. If a sapphire (0001) substrate is used, the film shows (100) orientations when its thickness is smaller than a critical value of about 60 nm. When the thickness exceeds the critical value, (101) oriented grains appear. This means that the (101) surface is stable under the given T and p_{O_2} . According to the present calculation, the experimental condition corresponds to the region in which the reduced (101) surface is most stable. Hence, this is consistent with the experimental results, although they did not examine the surface termination. Figure 2 shows the dependence of the critical

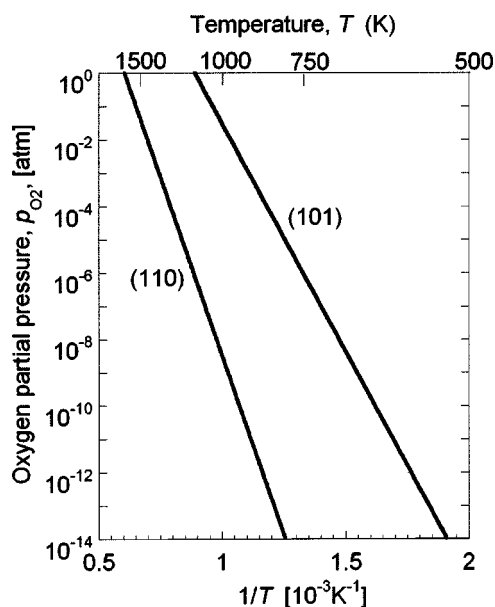


FIG. 2. Dependence of the critical temperature for redox between Sn_2O_4 (stoichiometric) and Sn_2O_2 (reduced) terminations on the oxygen partial pressure in the Arrhenius plot for the (110) and (101) surfaces.

temperature for the surface redox, T_c , on the oxygen partial pressure p_{O_2} in the Arrhenius plot. The diagram may be useful for process design of catalysis or gas sensors.

The geometries of four surfaces are shown in Fig. 3 with the corresponding layer relaxations in Table I. For the (110) surface, the relaxations are rather small and very similar between stoichiometric and reduced surfaces. Interestingly enough, the atomic relaxation is much more significant for

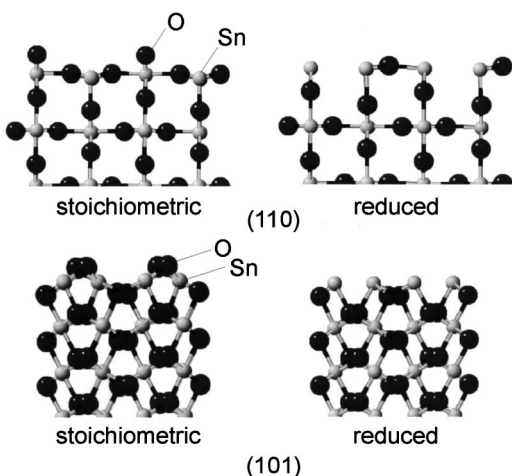


FIG. 3. Geometries of the four most stable surfaces: Stoichiometric Sn_2O_4 and reduced Sn_2O_2 (110) and (101) surfaces. The oxygen atoms are drawn in black; the tin atoms in gray.

TABLE I. Layer relaxation for the stoichiometric Sn_2O_4 and reduced Sn_2O_2 surfaces in % for (110) and (101).

110	Sn_2O_4	Sn_2O_2
O-Sn ₂ O ₂	-6.7	
Sn ₂ O ₂ -O	7.7	7.9
O-O	4.8	0.2
O-Sn ₂ O ₂	-1.0	0.1
Sn ₂ O ₂ -O	1.2	1.3
O-O	-3.4	-1.5
101	Sn_2O_4	Sn_2O_2
O ₂ -Sn ₂	9.4	
Sn ₂ -O ₂	-13.8	-4.2
O ₂ -O ₂	14.8	5.2
O ₂ -Sn ₂	-9.5	0.0
Sn ₂ -O ₂	0.2	-1.4
O ₂ -O ₂	1.0	1.6
O ₂ -Sn ₂	0.1	-0.4
Sn ₂ -O ₂	-1.5	-0.8
O ₂ -O ₂	1.7	1.2

the stoichiometric (101) surface, but is decreased by about two-thirds upon reduction of the surface.

In conclusion, we found that the reduced (101) surface of SnO_2 is the energetically most stable surface under conditions of high temperature or low p_{O_2} . This should play an important role in gas sensing and catalytic mechanisms. Although until now, the (110) surface has been extensively studied almost exclusively, the (101) surface should be very interesting and promising.

This work was supported by three projects from the Ministry of Education, Culture, Sports, Science, and Technology of Japan. They are a Grant-in-Aid for Scientific Research on Priority Areas (No. 751), the Computational Materials Science Project in Kyoto University, and the 21st century COE program.

- ¹J. Oviedo and M. J. Gillan, *Surf. Sci.* **490**, 221 (2001).
- ²F. R. Sensato, R. Custodio, M. Calatayud, A. Beltran, J. Andres, J. R. Sambrano, and E. Longo, *Surf. Sci.* **511**, 408 (2002).
- ³M. Batzill, K. Katsiev, and U. Diebold, *Surf. Sci.* **529**, 295 (2003).
- ⁴J. E. Dominguez, L. Fu, and X. Q. Pan, *Appl. Phys. Lett.* **79**, 614 (2001).
- ⁵J. E. Dominguez, X. Q. Pan, L. Fu, P. A. Van Rompay, Z. Zhang, J. A. Nees, and P. P. Pronko, *J. Appl. Phys.* **91**, 1060 (2002).
- ⁶Y. Wang and J. P. Perdew, *Phys. Rev. B* **44**, 13298 (1991).
- ⁷J. P. Perdew, J. A. Chevary, S. H. Vosko, K. A. Jackson, M. R. Pederson, D. J. Singh, and C. Fiolhais, *Phys. Rev. B* **46**, 6671 (1992).
- ⁸G. Kresse and J. Hafner, *Phys. Rev. B* **47**, 558 (1993).
- ⁹G. Kresse and J. Furthmüller, *Phys. Rev. B* **54**, 11169 (1996).
- ¹⁰G. Kresse and J. Furthmüller, *Comput. Mater. Sci.* **6**, 15 (1996).
- ¹¹P. E. Blöchl, *Phys. Rev. B* **50**, 17953 (1994).
- ¹²G. Kresse and J. Joubert, *Phys. Rev. B* **59**, 1758 (1999).
- ¹³K. Reuter and M. Scheffler, *Phys. Rev. B* **65**, 035406 (2001).
- ¹⁴D. R. Stull and H. Prophet, *JANAF Thermochemical Tables*, 2nd ed. (U.S. National Bureau of Standards, Washington, DC, 1971).
- ¹⁵J. Oviedo and M. J. Gillan, *Surf. Sci.* **463**, 93 (2000).
- ¹⁶M. A. Mäki-Jaskari and T. T. Rantala, *Phys. Rev. B* **65**, 245428 (2002).